AIP | Journal of Applied Physics

Axial ratio distribution effect of isolated microspheroids on the surface enhanced Raman scattering

L. C. Chu and Shou-yih Wang

Citation: Journal of Applied Physics **55**, 2776 (1984); doi: 10.1063/1.333285
View online: http://dx.doi.org/10.1063/1.333285
View Table of Contents: http://scitation.aip.org/content/aip/journal/jap/55/7?ver=pdfcov
Published by the AIP Publishing

Axial ratio distribution effect of isolated microspheroids on the surface enhanced Raman scattering

L. C. Chu
Institute of Electronics, National Chiao-Tung University, Hsinchu, Taiwan, Republic of China
Shou-yih Wang
Physics Department, National Tsing Hua University, Hsinchu, Taiwan 300, Republic of China

(Received 26 August 1983; accepted for publication 1 December 1983)

The surface enhanced Raman scattering as observed from molecules on Ag and Au arrays of microspheroids has been newly treated with suitable Gaussian distributions of axial ratios of these microspheroids. Calculated results for the enhancement factor features such as magnitude, peak position, and linewidth, all agree satisfactorily with existing experimental data, suggesting a possible physical mechanism for the Raman scattering.

PACS numbers: 78.30. − j, 68.20. + t, 78.20. − e

I. INTRODUCTION

Surface enhanced Raman scattering (SERS) has been widely studied ever since its first observation.[1] The enhancing mechanism or mechanisms provided by the noble metals Ag, Cu, Au, and a few weakly enhancing other metals has been proposed via various models.[2,3] The most extensively studied and also the most tractable one would be the electromagnetic model[4] which is based on essentially the enhancement of the incident field near the roughened metal surface. Along this line, the so-called particle plasmon (PP) model[5] appears to be rather powerful and convincing. It treats the local dipolar fields and thereby the SERS arising from isolated micro-objects, such as spheres or spheroids. The dielectric constant as a function of incident light frequency and the morphology of the particle gives essentially the particle plasmon resonance and the so-called lightning rod effect[6,7] respectively. The PP model was most clearly demonstrated by the well-known SERS experiments employing lithographically produced microstructures such as spheroids of Ag, Au, and Al regularly arranged in a two-dimensional array.[5,8] These experimental data obtained from the rather uniform size isolated micro-objects are certainly much more reproducible and tractable than those from an ordinarily roughened surface.

The original PP model, although very promising in SERS studies, will predict a resonance with the peak position and linewidth inconsistent with experiment. To state it more clearly, an electrostatic calcaulation using Gersten's[7] formulas for an Ag ellipsoid with the aspect ratio 3 : 1 will result in an energy peak position on the excitation profile quite apart from the experimental peak position as obtained in Ref. 5. For this problem, Wokaun, Gordon, Liao[9] and later Stern[8] introduced a radiation damping term $(i4\pi^2 V/3\lambda^3)$ along with the depolarization factor A. By least square fitting with the ellipsoidal volume V and A as two independent adjustable parameters they could approximately fit the excitation profile both for Ag and Au. However, this procedure is not entirely satisfactory simply because V and A should depend on each other. For instance, if we take the semiminor axis, $b = 50$ nm, which corresponds to the physical size of the top surface of the SiO_2 post, the aspect ratio of 3.8 : 1 (Ref. 5) gives $A = 0.081$ and simultaneously $V = 7.6\times10^{-15}$ cm^3 which largely deviates from the value[8] $V = 3.1\times10^{-16}$ cm^3. For the same purpose of understanding the SERS behavior from the lithographically produced micro-objects, Barber, Chang, and Massoudi[10,11] made a rigorous electrodynamical calculation of the SERS enhancement factor in various cases for Ag spheroids. Their electrodynamical results exhibit, among many other things, a shift of the main peak to longer wavelengths and broader linewidths, which are in the right direction to explain the features of the lithographically produced microstructures. Yet, as they have noted, the calculated peak position for Ag of aspect ratio 2 : 1 at 630 nm is different from the experimental position at 500 nm. Further, the calculated linewidth is about 2.5 times the experimental. At this point when the two important advances—radiation damping correction and electrodynamical calculation—are still not adequate for explaining SERS, the spheroids array problem itself appears to be quite involved. At the present stage of studies, one would like to investigate in detail each important aspect of the SERS problem. One would be the collective effect due to the coupling[10] among the arrayed spheriods. This is definitely a difficult topic. Another important aspect would be the effect due to the distribution of aspect ratios which will strongly affect both peak position and linewidth broadening. The purpose of this article is just to report the results from the statistical effect of the unavoidable distribution of aspect ratios of those lithographically produced spheriods of Ag and Au.

II. PHYSICAL JUSTIFICATION

Consider an isolated spheroid of semimajor axis a and semiminor axis b. The aspect ratios a/b or what we prefer to use here the reciprocal axial ratio $x = b/a$ for the Ag or Au micro-objects such as those in Refs. 5 and 8 must, in practice, have a distribution for each fabrication of such an array of micro-objects. A region illuminated by an incident laser light, say 0.5 mm in diameter, would cover more than 10^5 spheroids of $b = 50$ nm as the cases of Refs. 5 and 8. The Raman signal seen at the detector should reflect an average effect of the distributed axial ratios of these spheroids.

This phyical effect of the distribution over aspect ratios is itself interesting because it must be one of the true mechanisms which give the SERS behavior for those isolated spheroids. Further, the idea of the distribution would lead to the understanding of SERS of the general problem of roughened surface because the general roughness could possibly be replaced to give the same SERS results by a suitable distribution of size and morphology of closely arrayed isolated microstructures.

III. STATISTICAL FORMULATION

To treat the axial ratio distribution problem, we may regard the N spheroids as N independent measurements. Taking the reciprocal axial ratio of any one spheroid as a random variable s which has probability distribution $p(s)$, the sample mean of such N measurements is

$$x = \frac{1}{N}(s_1 + s_2 + \cdots + s_N).$$

According to the central limit theorem,[12] the distribution of the sample mean of a large number of measurements is Gaussian. Thus we assume a Gaussian type probability density function

$$f(x;m,v) = \frac{1}{\sqrt{2\pi v}} e^{-(x-m)^2/2v^2},$$

where m and v are the mean and the variance of the distribution, respectively. The averaged SERS enhancement is

$$\overline{R}(m,v) = \int R(x) f(x;m,v) dx,$$

where $R(x)$ is an expression for the SERS enhancement factor given by Gersten *et al.*[7,5] For the cases such as the Raman scattering from CN molecules on Ag where the laser frequency ω_L differs appreciably from the Stokes frequency ω_s, our expression for $R(x)$ is

$$R(x) = \left| 1 + \frac{[1-\epsilon(\omega_L)]\xi_0 Q_1'(\xi_1)}{\epsilon(\omega_L)Q_1(\xi_0) - \xi_0 Q_1'(\xi_0)} \right|^2 \times \left| 1 + \frac{[1-\epsilon(\omega_s)]\xi_0 Q_1'(\xi_0)}{\epsilon(\omega_s)Q_1(\xi_0) - \xi_0 Q_1'(\xi_0)} \right|^2,$$

in which the notations are referred to those of Eq. (4.10) of Ref. 7. The image factor $(1-\Gamma)$ in $R(x)$ is neglected because we place the molecule at a sufficiently large height, $H = 5$ Å above the tip of the spheroid.[7] For simplicity the average over the spheroidal surface is not calculated because the relevant features have been reported; these calculations give an average of about 1/6 of the peak value at the tip.[10,11] We choose the semimajor axis $a = 50$ nm in order to be consistent with the application of an electrostatic calculation.[7] Nevertheless, we note that, if using the electrostatic formulas of Ref. 7, the calculated results for three times larger value of a ($a = 150$ nm) yield essentially the same data for peak positions and linewidths.

IV. RESULTS AND DISCUSSION

Figure 1 shows the calculated SERS enhancement factor $\overline{R}(m;v)$ versus incident photon excitation energies for Au spheroids with $m = 1/3$ and various variances v. Clearly from this figure, the pure electrostatic calculation ($v = 0$) has

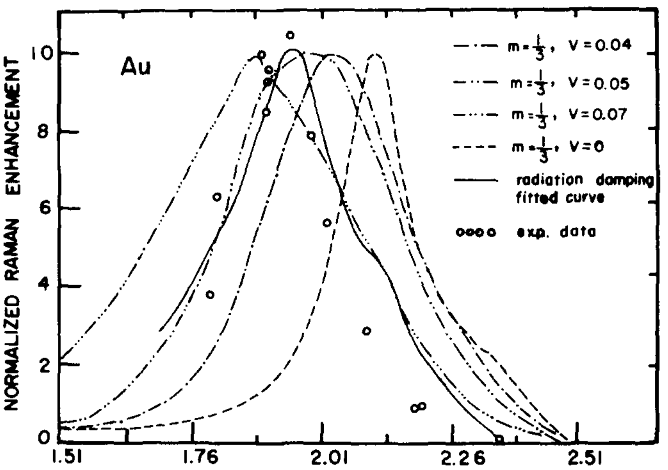

FIG. 1. Normalized enhancement factor for Au vs incident photon energies: $m = 1/3$ with various variances; solid line for radiation damping results cited from Ref. 9. Circles for experimental data.

both the peak position and the linewidth largely deviated from experimental data (open circles). The solid line is cited from Ref. 9 and represents the result of radiation damping. By gradually increasing the variance v the peak position shifts to longer wavelengths in a continuous manner. However, if v is so varied that the calculated peak positions approach the experimental peak, such as $v = 0.05$ and $v = 0.07$, the linewidths become too large and shapes of the peak become quite undesirable. The same situation will be more manifest for Ag in Fig. 3. This unnatural trend suggests to us that the true physical mean of the distribution is not 1/3. The depolarization factor A suggested in Ref. 8 as an adjustable parameter was 0.081.[8] The corresponding axial ratio is $m = 1/3.8$. In Fig. 2, the excitation curve with $m = 1/3.75$ *and* $v = 0.021$ is drawn to compare with the experimental data of Ref. 8. We believe $m = 1/3.75$ is closer to the truth from the view point of axial ratio distributions.

SERS enhancements for Ag spheroids are shown in

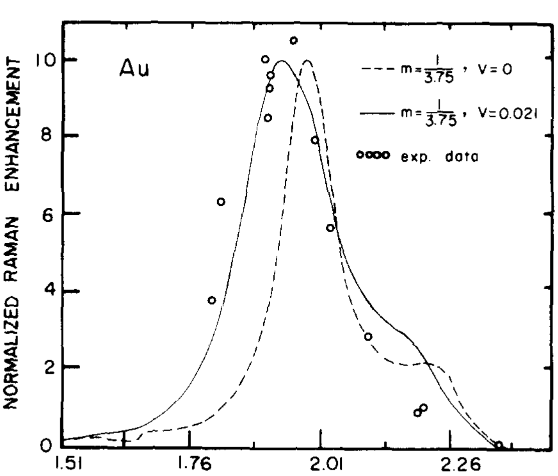

FIG. 2. Normalized enhancement factor for Au vs incident photon energies: $m = 1/3.75$, and $v = 0, 0.021$, showing the difference between a pure electrostatic calculation and that with some distribution. Circles for experimental data.

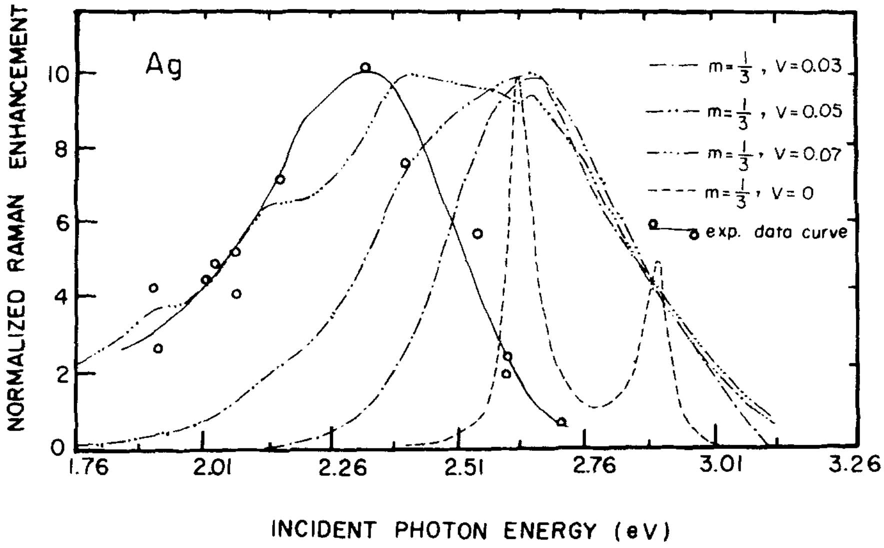

FIG. 3. Normalized enhancement factor for Ag vs incident photon energies with $m = 1/3$ and various variances. The solid line is just a smooth curve connecting the experimental data (circles).

Figs. 3, 4, and 5. In Fig. 3 we take $m = 1/3$ to meet the formal aspect ratio 3 : 1.[5] $\overline{R}\,(m,v)$ are drawn for variances 0, 0.03, 0.05, 0.07 to compare with the experimental curve. The curve for $v = 0$ shows two peaks, indicating those for laser frequency ω_L and Stokes frequency ω_s, respectively. This feature has been first mentioned in Ref. 5. The other curves with $v \neq 0$ exhibit linewidths which are too broad and which have undesirable shapes in comparison with the experimental data. As is in the case of Au, this situation should imply $m \neq 1/3$. To this, Ref. 5 states an aspect ratio 3.9 : 1 with 12% distribution (i.e., $v = 0.031$).

Using a distribution obtained from these parameters $m = 1/3.9$, $v = 0.031$ we plot $\overline{R}\,(m,v)$ in Fig. 4. The peak position and shorter wavelength side deviate considerably from experimental data. Further, there appears a shoulder at an incident photon energy of ~ 2.15 eV. We also plot $\overline{R}$ for 1/3.9 and $v = 0$. The peak position here is coincident with experiment, but two peaks emerge and thus can not agree with the experimental curve (solid line). This case demonstrates clearly the necessity of nonzero variance. In Fig. 5 we show the results for $m = 1/4.1$ with $v = 0.028$ which agree more satisfactorily. Again the $m = 1/4.1$, $v = 0$ case has two peaks and shows the necessity for $v \neq 0$.

As to the magnitude of the enhancement factors, we note that for Ag: $\overline{R}\,(m = 1/4.1,\ v = 0) = 1.04 \times 10^8$ for the larger peak (dashed line in Fig. 5) and $\overline{R}\,(m = 1/4.1,\ v = 0.028) = 3.51 \times 10^7$, are to be compared to the experimental enhancement of 10^7. Here we use $v = 0.028$ for the best fit of the experiment, as mentioned above. For Au: $\overline{R}\,(m = 1/3.75,\ v = 0) = 3.6 \times 10^6$ and $\overline{R}\,(m = 1/3.75,\ v = 0.021) = 3.05 \times 10^6$ are to be compared to an experimental enhancement of $\sim 10^6$. These appear rather reasonable. All the plots here are normalized to the experimental data to make the comparison of the peak positions and linewidths clear. About the two peaks for Ag (Figs. 3, 4, and 5) we note that these are not the multipole peaks as found in the electrodynamical calculation[10] because only dipolar resonances are concerned here.[7] These come from the appreciable separation (2144 cm^{-1}) between ω_L and ω_s as aforementioned. The absence of a second peak in the case of Au should result from the much larger value of the imaginary part of the dielectric constant $\epsilon_2(\omega)$ in comparison to that of Ag.[13] For aspect ratio

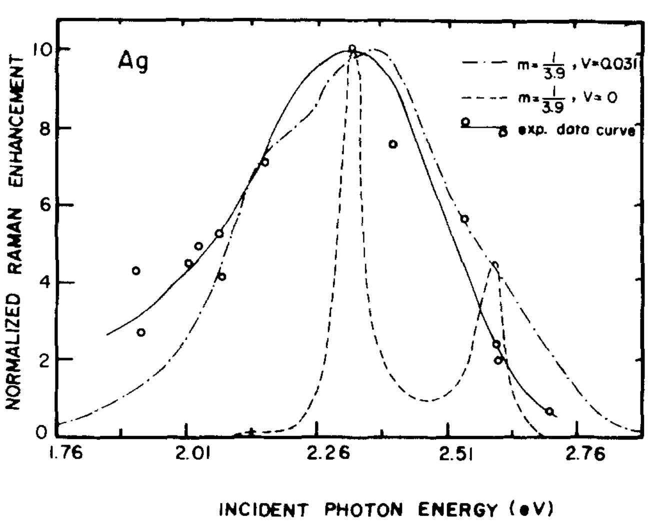

FIG. 4. Normalized enhancement factor for Ag vs incident photon energies: $m = 1/3.9$, $v = 0$, 0.031; solid line simply to connect experimental data; circles for experimental data.

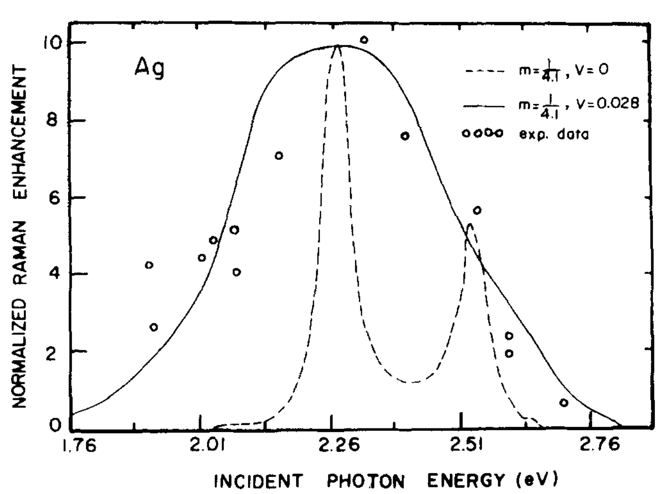

FIG. 5. Normalized enhancement factor for Ag vs incident photon energies: $m = 1/4.1$ and $v = 0$, 0.028; solid line is the calculated result from $v = 0.028$; circles for experimental data.

2 : 1 cases, which do not have available experimental data for Au, we find similar features as the 3 : 1 cases. These and other aspects, such as the effects of environments (air, water, or cyclohexane), are to be reported elsewhere.

In conclusion, we have for the first time in detail explored the physically unavoidable effect of the distribution over axial ratios of isolated microspheroids. The calculated enhancement factor itself could indicate whether the given formal axial ratios distribution is physically correct or not. The calculated results of magnitudes, peak positions and linewidths of the enhancement are in satisfactory agreement with existing experimental data, and tend to support the particle plasmon model for SERS.

ACKNOWLEDGMENTS

The authors wish to thank Mr. N. T. Liang, Dr. T. T. Chen, and Dr. Y. C. Chou for stimulating and helpful discussions.

[1]M. Fleischmann, P. J. Hendra, and A. J. McQuillan, Chem. Phys. Lett. **26**, 163 (1974).

[2]T. E. Furtak and J. Reyes, Surf. Sci. **93**, 35 (1980).

[3]For a review, see *Surface Enhanced Raman Scattering*, edited by R. K. Chang and T. W. Furtak (Plenum, New York, 1982).

[4]M. Moskovits, J. Chem. Phys. **69**, 4159 (1978); S. L. McCall, P. M. Platzman and P. A. Wolff, Phys. Lett. A **77**, 381 (1980).

[5]P. F. Liao, J. G. Bergman, D. S. Chemla, A. Wokaun, J. Melngailis, A. M. Hawryluk, and N. P. Bconomou, Chem. Phys. Lett. **82**, 355 (1981), and the references cited therein.

[6]J. Gersten, J. Chem. Phys. **72**, 5779 (1982); P. F. Liao and A. Wokaun, J. Chem. Phys. **76**, 751 (1982).

[7]J. Gersten and A. Nitzan, J. Chem. Phys. **73**, 3023 (1980).

[8]P. F. Liao and M. B. Stern, Opt. Lett. **7**, 483 (1982).

[9]A. Wokaun, J. P. Gordon, and P. F. Liao, Phys. Rev. Lett. **48**, 957 (1982).

[10]P. W. Barbar, R. K. Chang, and H. Massoudi, Phys. Rev. Lett. **50**, 997 (1983).

[11]P. W. Barbar, R. K. Chang, and H. Massoudi, Phys. Rev. B **27**, 7251 (1983).

[12]Jon Mathews and R. L. Walker, *Mathematical Methods of Physics*, 2nd ed. (Benjamin, New York, 1970).

[13]P. B. Johnson and R. W. Christy, Phys. Rev. B **6**, 4370 (1972).